

DUAL-BAND SIERPINSKI PRE-FRACTAL ANTENNA FOR 2.4 GHz-WLAN AND 800 MHz-LTE WIRELESS DEVICES

Federico Viani*

ELEDIA Research Group, Department of Information Engineering and Computer Science, University of Trento, Via Sommarive 14, Trento 38123, Italy

Abstract—A compact dual-band antenna for WLAN applications and Long Term Evolution (LTE) services in the 800 MHz band is designed. The compactness, the robustness, and the simplicity of the proposed solution make it suitable for the integration in recent and widely diffused mobile and multi-standard devices. The multiband behavior is yielded by exploiting a Sierpinski Gasket fractal shape whose descriptors are perturbed by means of a particle swarm optimization (PSO) strategy to fit the performance requirements. The results assess the good matching between numerical simulations and experimental validations as well as the effectiveness of the prototype in reaching a suitable impedance matching and satisfactory radiation characteristics.

1. INTRODUCTION

Nowadays, portable devices like smartphones and tablets integrate multiple wireless standards to enhance the connectivity and to enable heterogeneous services since more and more users are getting used to be often interconnected to wireless infrastructures allowing internet connections as well as voice calls. In such a framework and to provide even more fast and widespread connections, mobile terminals merge advantages of the WLAN technology with the new LTE standard for wireless data communications [1]. At the time of this writing, 285 operators in 93 different countries are investing in this latter evolution of the GSM/UMTS standards [2]. Many networks are under testing and operators interests and commitment are rapidly growing as recently experienced in Italy where telecommunication companies

Received 12 October 2012, Accepted 7 December 2012, Scheduled 11 December 2012

* Corresponding author: Federico Viani (federico.viani@disi.unitn.it).

awarded spectrum in the 800 MHz, 1800 MHz, and 2.6 GHz bands through a spectrum auction that raised a total price of Eur 3.9 billion. Since many frequency channels have been reserved for the frequency division duplex (FDD) LTE, ranging from the 700–800 MHz bands up to the 3500 MHz frequency bands, the design of reliable and efficient antenna systems for a so wide spectrum allocation is a big challenge especially when dealing with lower frequencies and the arising miniaturization problem for the integration in mobile devices. State of the art solutions have been mainly focused on the synthesis of radiating devices in the 700–800 MHz LTE bands also in conjunction with other mobile communication standards (e.g., GSM, GPRS, WiMAX, WLAN) for an integration in portable terminals [3–6]. However, finding the optimal trade-off among size, bandwidth, and efficiency at low frequencies is not a trivial task and many already proposed solutions suffer from narrow bandwidth [7] or too large size [8]. Alternatively, frequency-reconfigurable antennas excited by separate feeds for multiband operations [9, 10] turn out to be compact and with good performance at the cost of an increased hardware for the switch management. As for the multi-band behavior of single-feed structures, fractal geometries [11] proved their effectiveness in terms of flexibility (i.e., number and tuning of frequency bands), size reduction, and performances [12–22]. This is the motivation of proposing, in this letter, a simple and compact fractal monopole antenna covering the 2.4 GHz WLAN frequency band (2400–2480 MHz) and the LTE5 (824–894 MHz), LTE6 (830–885 MHz), LTE18 (815–875 MHz), LTE19 (830–890 MHz), and LTE20 (791–862 MHz) channels. The paper is organized as follows. Section 2 describes the proposed antenna geometry and a selected set of numerical and experimental results are presented in Section 3. Finally, some concluding remarks are drawn in Section 4.

2. ANTENNA DESIGN

The antenna geometry is defined through the control parameter vector $\alpha = (h_A, w_A, h_F, w_F, l_n; n = 1, \dots, 3)$, where h_A and w_A are the total height and width of the antenna substrate, respectively, while h_F and w_F univocally determine the feeding section as shown in Fig. 1(a). Concerning the geometry of the fractal radiating element, the Sierpinski Gasket fractal iteration index $j = 0, \dots, J$ has been stopped to $J = 1$ and the dual-band behavior has been obtained by acting on the parameters $l_n; n = 1, \dots, 3$ (Fig. 1) through the PSO-based optimization strategy presented in [23]. More specifically, the antenna behavior has been numerically simulated with

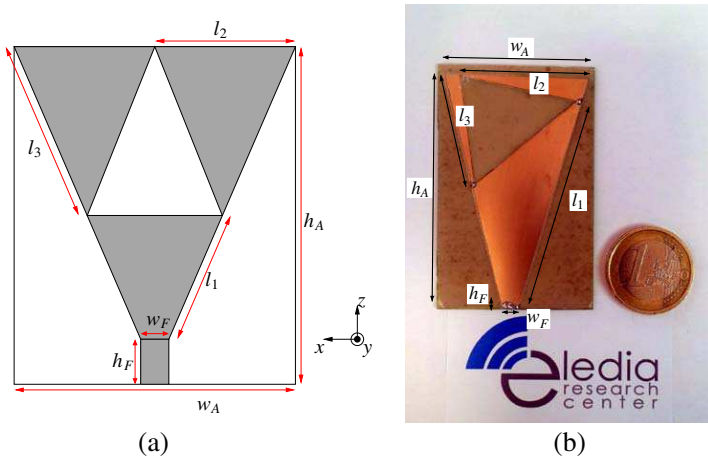


Figure 1. Sierpinski fractal antenna prototype.

a standard MoM-based electromagnetic simulator [24] and the PSO-based optimization strategy has been exploited to identify the antenna geometry able to satisfy the following requirements on the impedance matching

$$S_{11}(f) \leq \begin{cases} S_{11}^{th\alpha} & f = f_i; i = 1, 2 \\ S_{11}^{th\beta} & f \in [f_{\min} \div f_{\max}]^{(i)}; i = 1, 2 \end{cases} \quad (1)$$

where $S_{11}^{th\alpha}$ is the threshold of the desired S_{11} scattering parameter at the center frequencies $f_1 = 854.5$ MHz and $f_2 = 2440$ MHz, and $S_{11}^{th\beta}$ is the threshold related to the frequency bands limits f_{\min} and f_{\max} . In particular, the first ($i = 1$) band ranges from $f_{\min}^{(1)} = 815$ MHz up to $f_{\max}^{(1)} = 894$ MHz, while the higher WLAN band extends from $f_{\min}^{(2)} = 2400$ MHz up to $f_{\max}^{(2)} = 2483.5$ MHz. In order to fit those specifications, the synthesis procedure has been aimed at minimizing the following cost function

$$\Omega(\delta) = \sum_i \left\{ \frac{\max \left[0, \frac{S_{11}(f_i) - S_{11}^{th\alpha}}{S_{11}^{th\alpha}} \right]}{f_i} + \frac{\int_{f_{\min}^i}^{f_{\max}^i} \max \left[0, \frac{S_{11}(f) - S_{11}^{th\beta}}{S_{11}^{th\beta}} \right] df}{f_{\max}^i - f_{\min}^i} \right\}. \quad (2)$$

where $S_{11}^{th\alpha} = -10$ dB and $S_{11}^{th\beta} = -8$ dB. Besides the impedance matching constraints, suitable geometrical limits have been imposed on the antenna size (i.e., $h_A^{MAX} = 70$ mm and $w_A^{MAX} = 45$ mm) to guarantee a high integrability in portable devices.

In order to find the optimal solution, the optimization algorithm updates at each iteration the trial solutions $\delta_p^{(k)}$; $p = 1, \dots, P$; $k = 1, \dots, K$, where P and K are the dimension of the swarm and the maximum number of iterations, respectively. During the optimization process, the swarm explores the solution space updating the corresponding particle velocities $v_p^{(k)}$; $p = 1, \dots, P$ according to the following equation [25]

$$v_p^{(k+1)} = \omega v_p^{(k)} + C_1 \lambda_1 \left(\delta_{pbest,p}^{(k)} - \delta_p^{(k)} \right) + C_2 \lambda_2 \left(\delta_{gbest}^{(k)} - \delta_p^{(k)} \right) \quad (3)$$

where ω is the inertial weight, and C_1 and C_2 are the cognitive and social acceleration indexes, respectively. Moreover, λ_1 and λ_2 are random variables uniformly distributed in the range $[0 : 1]$. Furthermore, $\delta_{pbest,p}^{(k)} = \arg\{\min_{i=1,\dots,k} [\Omega(\delta_p^{(i)})]\}$; $p = 1, \dots, P$ is the *personal best* solution found by each p -th particle, and $\delta_{gbest}^{(k)} = \arg\{\min_{i=1,\dots,k; p=1,\dots,P} [\Omega(\delta_p^{(i)})]\}$ is the *global best* solution until the k -th iteration. The optimization has been carried out setting the PSO control parameters $\omega = 0.7$, $C_1 = 2.0$, and $C_2 = 2.0$, as suggested in [25]. The dimension of the PSO swarm has been set to $P = 8$ and the maximum number of iterations to $K = 100$. At the convergence, $k = 56$, (i.e., the value of the optimized cost function lower than a the convergence threshold $\sigma = 10^{-5}$) the optimal configuration turned out to be characterized by: $h_A = 66$ mm, $w_A = 41$ mm, $h_F = 0.5$ mm, $w_F = 5$ mm, $l_1 = 61.54$ mm, $l_2 = 36.98$ mm, and $l_3 = 33.17$ mm.

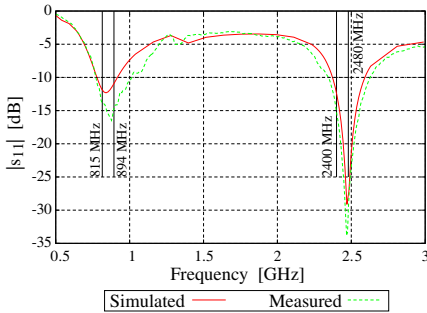


Figure 2. Plots of the simulated and measured reflection coefficient in terms of S_{11} scattering parameter over the considered frequency range.

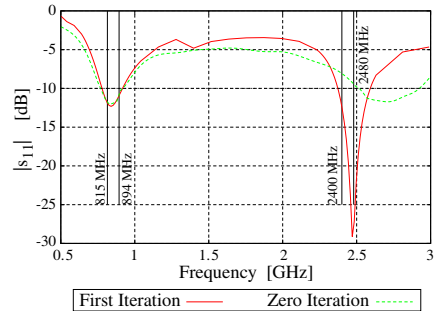


Figure 3. Comparison of the simulated S_{11} for the zero iteration and first iteration fractal antennas.

3. NUMERICAL AND EXPERIMENTAL VALIDATION

The radiation properties of the synthesized antenna have been numerically and experimentally verified. Towards this end, an antenna prototype has been realized with a photolithographic printing circuit technology on an Arlon substrate with thickness 0.8 mm and dielectric characteristics $\epsilon_r = 3.38$ and $\tan \delta = 2.5 \times 10^{-3}$ [Fig. 1(b)]. The measurements concerning impedance matching and radiation patterns have been performed in an anechoic chamber where the antenna radiator has been mounted on a metallic ground plane and connected to the measurement setup through a coaxial cable and 50Ω SMA connectors. As for the electrical performances, Fig. 2 shows the behavior of the simulated and measured reflection coefficient in terms of scattering parameter S_{11} within the frequency range $f \in [500 \div 3000]$ MHz. As it can be observed, there is a good agreement between the two plots and the resonances turn out to be clearly tuned at the desired frequency bands. Compared to other state of the art solutions, where small antennas exhibit narrow bandwidths, the bandwidths at hand are wide enough even though the antenna maximum length is 25% smaller than a standard quarter-wave monopole at f_1 . In order to point out the potentialities of the adopted first-order fractal geometry in matching the two required resonances, the obtained antenna has been compared with the zero-order fractal geometry (i.e., stopping the Sierpinski Gasket fractal generator to the zero iteration). The two simulated scattering parameter S_{11} have been compared as shown in Fig. 3. As expected, the first resonance, mainly related to the external

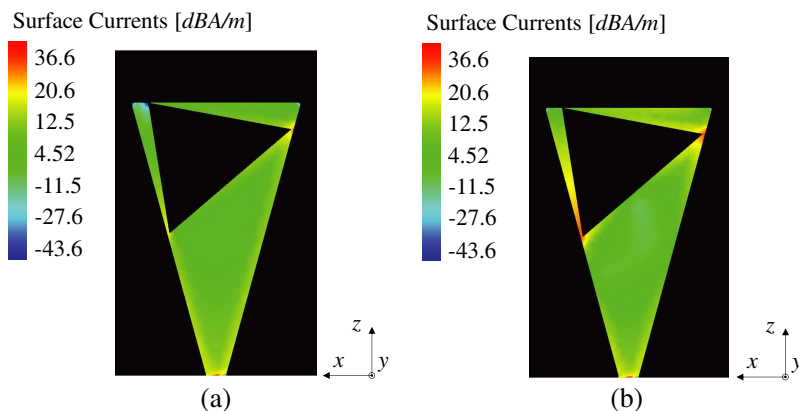


Figure 4. Surface current distributions at center working frequencies (a) $f_1 = 854.5$ MHz and (b) $f_2 = 2440$ MHz.

Sierpinski triangle, remains unchanged for both antenna geometries, while the second one turns out to be more controlled by the inner and smaller Sierpinski triangle, and consequently it is not correctly matched by the zero iteration fractal radiator.

The surface current distributions at the two center frequencies are graphically shown in Fig. 4. They further confirm the dual-band behavior of the fractal radiator pointing out a strict relation with the geometrical characteristics of the Sierpinski descriptor. It is worth to be noticed that the perturbed triangle related to the first fractal iteration is responsible for the antenna radiation at the second working frequency f_2 , as graphically confirmed by the higher current values (respect to the currents behavior at the lower frequency f_1) close to the inner triangle vertices.

As far as the radiation properties are concerned, the three-dimensional representations for the radiation patterns at frequencies f_1 and f_2 are shown in Fig. 5. With the aim of comparison with measurements, Fig. 6 shows the two-dimensional cuts along the horizontal and vertical planes. The arising patterns present characteristics similar to those of a standard monopole antenna, even though some secondary lobes appear at the WLAN frequency band because of the presence of the ground plane. Nevertheless, the antenna prototype turns out to be suitable for WLAN and LTE applications thanks to the omnidirectional behavior along the horizontal plane at the considered frequency bands. Moreover, the radiation efficiency turns out to be very high in both bands: $\rho(f_1) = 97.1\%$ and $\rho(f_2) = 92.4\%$.

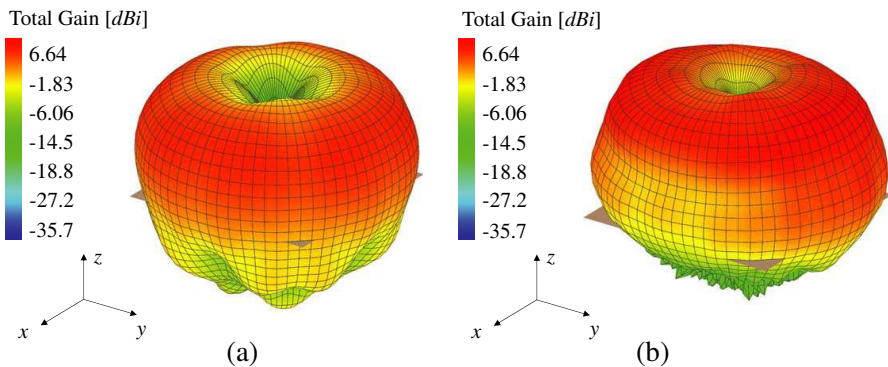


Figure 5. Three-dimensional representation of radiation patterns at (a) $f_1 = 854.5$ MHz and (b) $f_2 = 2440$ MHz.

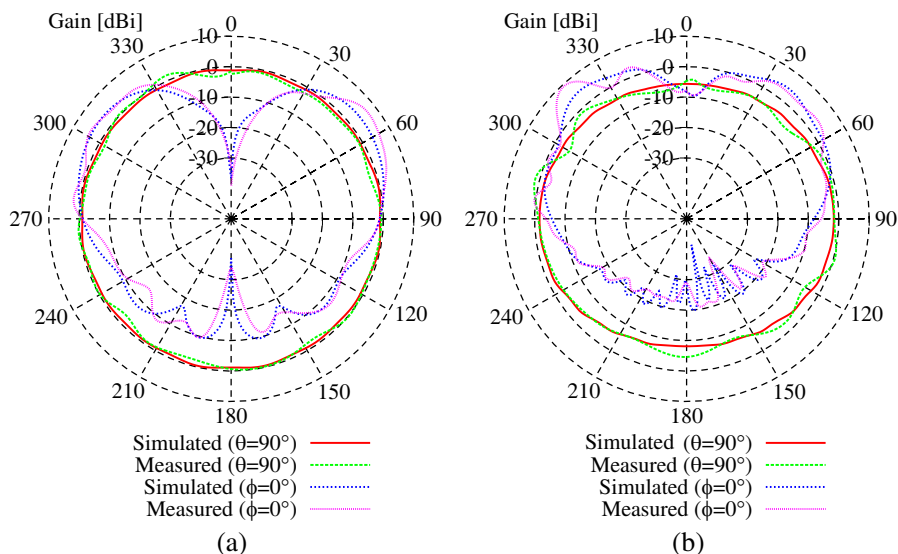


Figure 6. Horizontal ($\theta = 90^\circ$) and vertical ($\phi = 0^\circ$) cuts of the simulated and measured radiation patterns at the (a) 800 MHz LTE band and the (b) 2.4 GHz WLAN band.

4. CONCLUSIONS

In this paper, a multiband antenna based on the Sierpinsky Gasket fractal descriptor shape has been proposed for WLAN and 800 MHz LTE mobile standards. The antenna geometry has been synthesized by means of a PSO-based optimization to satisfy suitable performance requirements. The synthesized solution has been numerically and experimentally assessed. The results clearly point out the effectiveness of the antenna prototype in terms of impedance matching, radiation properties, and efficiency.

REFERENCES

1. Sesia, S., I. Toufik, and M. Baker, *LTE — The UMTS Long Term Evolution: From Theory to Practice*, Wiley, Chichester, UK, 2009.
2. GSA Evolution to LTE report, Jan. 2012, (http://www.gsacom.com/gsm_3g/info_papers).
3. Xiong, J.-P., L. Liu, X.-M. Wang, J. Chen, and Y.-L. Zhao, "Dual-band printed bent slots antenna for WLAN applications," *Journal of Electromagnetic Waves and Applications*, Vol. 22, Nos. 11–12, 1509–1515, 2008.

4. He, K., R.-X. Wang, Y.-F. Wang, and B.-H. Sun, "Compact tri-band claw-shaped monopole antenna for wlan/wimax applications," *Journal of Electromagnetic Waves and Applications*, Vol. 25, Nos. 5–6, 869–877, 2011.
5. Lee, J. N. and J. K. Park, "Design of multi-band antenna with F-shaped slot," *Journal of Electromagnetic Waves and Applications*, Vol. 24, Nos. 2–3, 179–188, 2010.
6. Cheng, P.-C., C.-Y.-D. Sim, and C.-H. Lee, "Multi-band printed internal monopole antenna for mobile handset applications," *Journal of Electromagnetic Waves and Applications*, Vol. 23, No. 13, 1733–1744, 2009.
7. Kan, H. K. and R. B. Waterhouse, "Shorted spiral like printed antennas," *IEEE Trans. on Antennas and Propag.*, Vol. 59, No. 3, 396–397, 2002.
8. Wang, G., J. Liu, J. Xia, and L. Yang, "Coaxial-fed double-sided bow-tie antenna for GSM/CDMA and 3G/WLAN communications," *IEEE Trans. on Antennas and Propag.*, Vol. 56, No. 8, 2739–2742, 2008.
9. Cho, J., C. W. Jung, and K. Kim, "Frequency-reconfigurable two-port antenna for mobile phone operating over multiple service band," *Electron. Lett.*, Vol. 45, No. 20, 1009–1011, 2009.
10. Ouyang, J., F. Yang, Z. P. Nie, and Z. Q. Zhao, "A novel frequency reconfigurable microstrip antenna for wideband application," *Journal of Electromagnetic Waves and Applications*, Vol. 22, No. 10, 1403–1410, 2008.
11. Puente-Baliarda, C., J. Romeu, R. Pous, and A. Cardama, "On the behavior of the Sierpinski multiband fractal antenna," *IEEE Trans. on Antennas and Propag.*, Vol. 46, No. 4, 517–524, 1998.
12. Viani, F., M. Salucci, F. Robol, G. Oliveri, and A. Massa, "Design of a UHF RFID/GPS fractal antenna for logistics management," *Journal of Electromagnetic Waves and Applications*, Vol. 26, No. 4, 480–492, 2012.
13. Viani, F., M. Salucci, F. Robol, and A. Massa, "Multiband fractal Zigbee/WLAN antenna for ubiquitous wireless environments," *Journal of Electromagnetic Waves and Applications*, Vol. 26, Nos. 11–12, 1554–1562, Aug. 2012.
14. Karim, M. N. A., M. K. Abd Rahim, H. A. Majid, O. B. Ayop, M. Abu, and F. Zubir, "Log periodic fractal koch antenna for UHF band applications," *Progress In Electromagnetics Research*, Vol. 100, 201–218, 2010.
15. Li, D. and J.-F. Mao, "Koch-like sided Sierpinski gasket

- multifractal dipole antenna,” *Progress In Electromagnetics Research*, Vol. 126, 399–427, 2012.
16. Anguera, J., J. P. Daniel, C. Borja, J. Mumbru, C. Puente, T. Leduc, K. Sayegrih, and P. Van Roy, “Metallized foams for antenna design: Application to fractal-shaped Sierpinski-carpet monopole,” *Progress In Electromagnetics Research*, Vol. 104, 239–251, 2010.
 17. Xu, H.-Y., H. Zhang, X. Yin, and K. Lu, “Ultra-wideband koch fractal antenna with low backscattering cross section,” *Journal of Electromagnetic Waves and Applications*, Vol. 24, Nos. 17–18, 2615–2623, 2010.
 18. Siakavara, K., “Novel fractal antenna arrays for satellite networks: Circular ring Sierpinski carpet arrays optimized by genetic algorithms,” *Progress In Electromagnetics Research*, Vol. 103, 115–138, 2010.
 19. Lizzi, L., F. Viani, E. Zeni, and A. Massa, “A DVBH/GSM/UMTS planar antenna for multimode wireless devices,” *IEEE Antennas Wireless Propag. Lett.*, Vol. 8, 568–571, 2009.
 20. Azaro, R., F. Viani, L. Lizzi, E. Zeni, and A. Massa, “A monopolar quad-band antenna based on a Hilbert self-affine prefractal geometry,” *IEEE Antennas Wireless Propag. Lett.*, Vol. 8, 177–180, 2008.
 21. Lizzi, L., R. Azaro, G. Oliveri, and A. Massa, “Multiband fractal antenna for wireless communication systems for emergency management,” *Journal of Electromagnetic Waves and Applications*, Vol. 26, No. 1, 1–11, 2012.
 22. Naghshvarian-Jahromi, M., “Novel miniature semi-circular-semi-fractal monopole dual band antenna,” *Journal of Electromagnetic Waves and Applications*, Vol. 22, Nos. 2–3, 227–237, 2008.
 23. Azaro, R., F. De Natale, M. Donelli, E. Zeni, and A. Massa, “Synthesis of a prefractal dual-band monopolar antenna for GPS applications,” *IEEE Antennas Wireless Propag. Lett.*, Vol. 5, No. 1, 361–364, 2006.
 24. Harrington, R. F., *Field Computation by Moment Methods*, Robert E. Krieger, Malabar, FL, 1987.
 25. Robinson, J. and Y. Rahmat-Samii, “Particle swarm optimization in electromagnetics,” *IEEE Trans. on Antennas and Propag.*, Vol. 52, No. 2, 397–407, Feb. 2004.